

SPIRAL INFLECTORS AND ELECTRODES IN THE CENTRAL REGION OF THE VINCY CYCLOTRON

P. Beličev, V. Jocić, N. Nešković, B. Rađenović, M. Rajčević, Laboratory of Physics, Vinča Institute of Nuclear Sciences, Belgrade, Serbia

E. E. Perepelkin, A. S. Vorozhtsov, S. B. Vorozhtsov, Dzhelepov Laboratory of Nuclear Problems, Joint Institute for Nuclear Research, Dubna, Russia

Abstract

The initial design of the electrodes in the central region of the VINCY Cyclotron assumed the maximal amplitude of the accelerating voltage of 100 kV, for acceleration of the H^- ion beam up to the energy of 65 MeV. Due to the small gaps between the biased and grounded electrodes, such a high voltage would result in a high sparking probability, which would be unfavorable for proton therapy, being one of the programs of use of the machine. In order to overcome this problem, we have redesigned the electrodes. The main objective was to decrease the maximal amplitude of the accelerating voltage down to about 70 kV. Here, the new design of the electrodes as well as of the corresponding spiral inflectors is presented. It has resulted from calculations of the beam transport in the central and acceleration regions of the machine for its test beams, which are the H^- beam accelerated up to 65 MeV, the H_2^+ beam accelerated up to 60 MeV, the $^4He^+$ beam accelerated up to 28 MeV, and the $^{40}Ar^{6+}$ beam accelerated up to 120 MeV. They were performed using the CBDA [1], COMSOL [2] and TOSCA [3] computer codes.

INTRODUCTION

The VINCY Cyclotron is a room temperature isochronous cyclotron meant to accelerate both light and multiply charged heavy ions, operating with the harmonic number of the accelerating voltage $h = 1, 2, 3$ and 4. The corresponding test ion beams are the H^- , H_2^+ , $^4He^+$ and $^{40}Ar^{6+}$ beams, to be accelerated up to the energies of 65, 60, 28 and 120 MeV, respectively. These ranges of ion masses and charges are quite demanding with respect to the electrode configuration in the central region of the machine, especially if one wants to avoid movable parts and keep it as simple as possible.

Injection of the beams is performed via four spiral inflectors, corresponding to the four values of the harmonic number (h). In order to provide their proper centring and acceleration, the beams are allowed to enter the central region through one of the two openings on the opposite sides of the inflector housing.

The main goals in determining the shapes of the electrodes in the central region were: to center the beam properly up to its extraction radius, to keep the amplitude of the accelerating voltage below about 70 kV, and to minimize the beam losses.

Our previous calculations showed that the H^- and H_2^+ beams, which are accelerated with $h = 1$ and 2, respectively, and the $^4He^+$ and $^{40}Ar^{6+}$ beams, which are

accelerated with $h = 3$ and 4, respectively, should exit from the inflector housing through the openings on its opposite sides.

OPTIMIZATION ALGORITHM

The main restriction in designing the electrodes in the central region is the fact that the dee-antidee structure of the radiofrequency system (RF) of the machine has already been manufactured. Therefore, only the space up to the radius of 6 cm is available. The optimization algorithm starts with backtracking the referent particle from its extraction radius to the radius of about 6 cm. Further, the referent particle is backtracked to one of the openings of the inflector housing for different positions of the accelerating gaps, in order to place them in the optimal way. In these calculations one must check if the final referent particle energy, E_{inj} , at the opening is below the maximal injection energy. For the H^- , H_2^+ and $^4He^+$ beams, which are produced by a multicusp ion source, the maximal injection voltage is 30 kV, while for the $^{40}Ar^{6+}$ beam, which is produced by an ECR ion source, it is 25 kV. We created a data base of the numerically calculated electric fields in the two types of accelerating gaps, with the posts and without them. They are shown in Fig. 1.

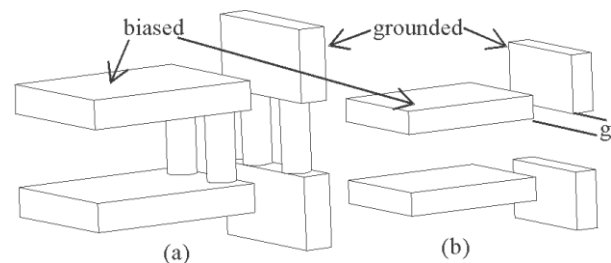


Figure 1: A sketch of the two types of accelerating gaps used in the optimization algorithm: (a) with the posts and (b) without the posts; g is the horizontal gap size.

The electric field in a gap can be expressed as a function of six parameters, $\mathbf{E}(x, y, r_C, \varphi_C, \varphi, g, p)$, where (x, y) are the rectangular coordinates of a point in the gap coordinate system, (r_C, φ_C) are the polar coordinates of the gap centre in the coordinate system of the machine, φ determines the gap orientation in the median plane of the machine, g is the horizontal gap size, and p is the indicator of the type of accelerating gap. The optimal positions of the gaps are found by minimizing functional $F(r_C, \varphi_C, \varphi, g, p) = U_{RF}Ze - W_g$, where Ze is the referent particle charge, U_{RF} the amplitude of the accelerating

voltage, and W_g the energy gain of the referent particle in the gap. Thus, we obtain the maximal energy gain in all the gaps. The strict application of the optimization algorithm would lead to the angular spans between the two successive gaps equal to 180, 90, 60 and 45 deg for $h = 1, 2, 3$ and 4, respectively.

RESULTS

Unfortunately, these gap positions cannot be successfully unified into a joint configuration. In order to overcome this difficulty, we imposed the additional restrictions that the angular span between the two successive gaps must be smaller than 90 deg for $h = 1$ and 2, and smaller than 45 deg for $h = 3$ and 4.

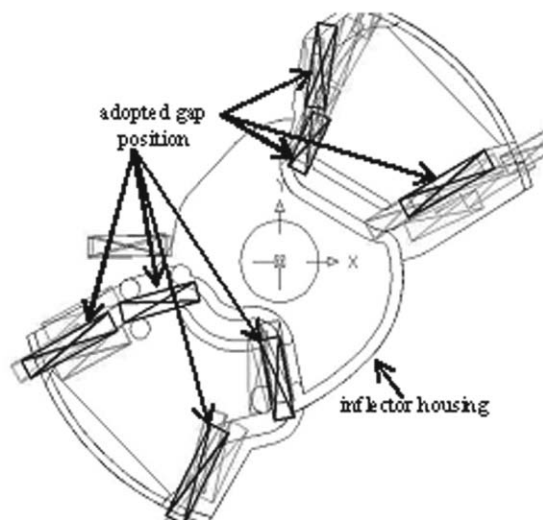


Figure 2: The optimal positions of the gaps for different referent particles – thin crossed rectangles, and the adopted positions of the gaps for all the referent particles – thick crossed rectangles.

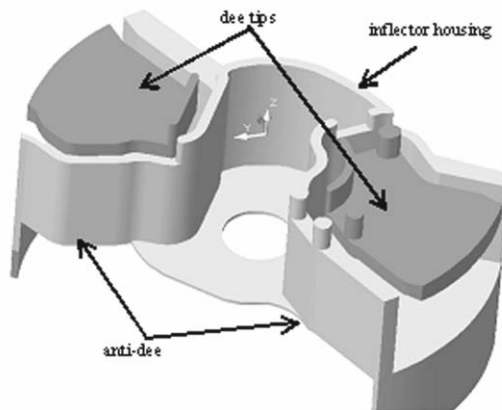


Figure 3: A 3D model of the electrodes in the central region (the part below the median plane).

The obtained optimal positions of the gaps for different referent particles and the adopted positions of the gaps for all the referent particles are shown in Fig. 2. The latter positions were obtained by averaging the former positions. We started from the adopted positions of the gaps and created a three-dimensional (3D) model of the electrodes in the central region. It is given in Fig. 3. The corresponding 3D electric field map was calculated using the COMSOL and TOSCA computer codes [2, 3]. In order to check the quality of the obtained electrode configuration, the final parameters of the referent particles in the backtracking calculations were used as the initial parameters in the forward tracking calculations. These parameters are given in Table 1. The results of these beam transport simulations, performed by the CBDA code [1], are presented in Fig. 4. The initial horizontal and vertical beam emittances used in these calculations were 50 and 260 π -mm-mrad, respectively. The isolated dots in the figure represent the beam losses on the electrodes, reaching 28 and 14 % for the H^- and H_2^+ beams, respectively, and being zero for the $^4He^+$ and $^{40}Ar^{6+}$ beams. Using the obtained initial parameters of the four referent particles we defined the corresponding four spiral inflectors. Their parameters are given in Table 2, where R_m , A and V stand for the inflector magnetic radius, electric radius and biasing potential, respectively. The question of optimization of the fringe electric fields in the inflectors, by cutting its electrodes and/or their asymmetric biasing, in order to obtain the properly centered beams at their exits is yet to be solved.

CONCLUSIONS

In order to avoid the accelerating voltage of about 100 kV in the initial electrode configuration, a new one was successfully designed. The optimization algorithm was based on the referent particle backtracking and maximization of its energy gain in the gaps, whose positions were varied. It contained the additional restrictions related to the particle injection energy, the available space and the angular spans between the successive gaps. The electric fields used in the calculations were obtained using a data base of the numerically calculated maps for two types of gaps (with the posts and without them) with variable parameters. After obtaining the optimal positions of the gaps for each test beam, the final positions of the gaps for all the test beams were adopted. A detailed 3D model of the adopted electrode configuration was created and the corresponding electric field map was calculated. The beam transport simulations showed that the adopted electrode configuration allows the successful acceleration of all the test beams with the accelerating voltage not exceeding 72 kV, what was our goal. Besides, the beam losses in the central region due to the collisions with the electrodes are minimized, except in the case of H^- beam, when they reached 28 %. The spiral inflectors for all the test beams were defined as well.

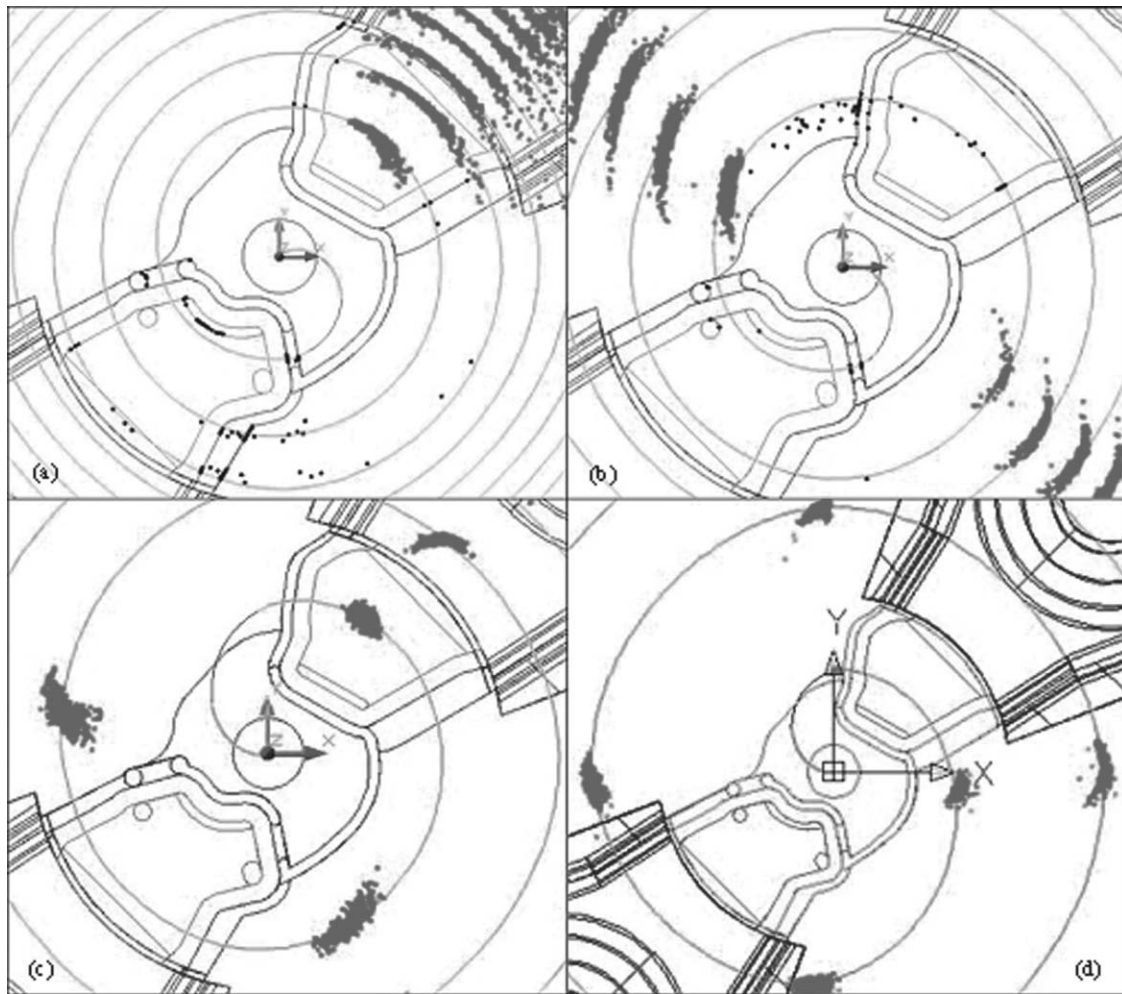


Figure 4: The results of the beam transport simulations in the adopted electrode configuration for (a) H^- beam, (b) H_2^+ beam, (c) ${}^4\text{He}^+$ beam, and (d) ${}^{40}\text{Ar}^{6+}$ beam. The isolated dots in (a) and (b) represent the beam losses on the electrodes.

Table 1: The initial parameters of the referent particles

Ion	E_{inj} [KeV]	U_{RF} [kV]	Initial RF phase [deg]	RF frequency [MHz]	Initial radius [mm]	Initial azimuthal angle [deg]	Initial radial direction [deg]
H^-	26.585	72	14	20.038	26.4	-68.4	15.5
H_2^+	17.7	65	-42.6	28.006	24.9	-69.9	27.35
${}^4\text{He}^+$	28.1	50	106.3	20.7	40	95.1	26.4
${}^{40}\text{Ar}^{6+}$	72.33	70	-148.1	18.163	37	95.6	16.8

Table 2: The parameters of the spiral inflectors

Parameters	H^-	H_2^+	${}^4\text{He}^+$	${}^{40}\text{Ar}^{6+}$
Tilt	0.4795	0.118	0.3532	-0.0244
R_m [mm]	18.17	16.5	26.389	20.315
A [mm]	25	25	25	25
V [kV]	± 8.5	± 5.665	± 8.979	± 3.858

REFERENCES

- [1] E. E. Perepelkin, A. S. Vorozhtsov, S. B. Vorozhtsov and L. M. Onischenko, XX Russian Particle Accelerator Conference (RuPAC 2006), Novosibirsk, September 10-14, 2006, p. 348.
- [2] COMSOL Multiphysics Modeling Software, <http://www.comsol.com>.
- [3] TOSCA Reference Manual, Vector Fields, Oxford, UK.